Fractional Calculus & Applied Analysis
An International Journal for Theory and Applications
VOLUME 12, NUMBER 4 (2009) ISSN 1311-0454

BOND GRAPH PRIMITIVES FOR MODELING SYSTEMS WITH FRACTIONAL DIFFERENTIAL EQUATIONS

Thomas J. Connolly [1], **Jaime A. Contréras** [2]

Abstract

This paper presents a new simulation approach for dynamical systems that results from the extension of the bond graph methodology to the modeling of systems where the behaviors of one or more components are dictated by a fractional derivative. We present two new primitive elements, and demonstrate their necessity in modeling systems that contain such components using impedance-based bond graphs. The introduction of these primitive elements effectively extends the utility of the bond graph method to include physical phenomena that are more accurately modeled using fractional derivatives. Further, the application of bond graphs to example systems facilitated the development of a new approach in the numerical solution of the state equations, i.e., the conceptualization of a hybrid (fractional and integer-order) state space. Example applications presented in this paper involve systems where viscoelastic and viscoinertial phenomena are present. Simulation results demonstrate the validity of the hybrid state-space approach. They also demonstrate how the introduction of fractional-calculus based primitives broadens the range of systems that can be modeled using single-port bond graph models, thus expanding the use of fractional calculus concepts to a wider audience in the dynamical systems modeling community.

2000 Mathematics Subject Classifications: 26A33, 62P30, 70G60, 93A30

Key Words and Phrases: fractional derivative, bond graph, impedance, dynamical system

1. Introduction

This paper introduces new bond primitives, and a new computational approach borne out of their application, for complex physical phenomena whose constitutive behaviors can be modeled using fractional derivatives [6], [7]. Such constructs find practical application in the modeling of viscoelastic and viscoinertial effects that are encountered in the modeling and control of complex engineering systems.

The first objective of this paper is to formulate and justify the necessity of two new primitive bond graph elements that represent constitutive behaviors governed by fractional derivatives. The second objective is to demonstrate the utility of these new primitive elements in modeling dynamical systems that exhibit phenomena which cannot be modeled using existing bond graph constructs. The third objective is to introduce the notion of a hybrid fractional/integer-order state space, which facilitates numerical solution of the system of differential equations that are derived from a bond graph model which contains a fractional-order primitive element.

A short overview of bond graph theory, and its application to impedance-based modeling of dynamical systems in the frequency domain, is presented. Next, primitive bond graph elements that represent physical phenomena that can be modeled using fractional derivatives, are proposed. Arguments that support the necessity of such elements are developed using complex-plane representations and equivalent impedance relations.

Practical applications of fractional derivatives in the modeling of viscoelastic and viscoiniertial effects in dynamical systems are cited and then cast into a bond graph framework that includes fractional-order primitives. An example problem that illustrates the utility of the new primitive elements in dynamical system modeling and analysis is then presented. Within the context of this problem, a new computational approach for solving systems of differential equations that contain both integer-order and fractional-order derivatives, is presented and validated.

2. Bond graph overview

The bond graph methodology is a modeling tool for physical systems that involve one or more energy domains, i.e., mechanical, electrical, fluidic, etc. Bond graphs map the power flow between the interconnected elements of a system, which either store or dissipate energy, or transform energy from one energy domain to another. In addition to representing the topology of a system, bond graphs facilitate the derivation of the system of differential

equations that describe the behavior of a dynamical system. This section provides a brief overview of the bond graph method and is limited to the scope of this paper. For detailed treatments of the bond graph method, see [4], [10].

Primitive Elements

The basic building block of a bond graph model is shown in Figure 1, where the half-arrow is called a *power bond* and **S** represents a generic element of a system. Power is represented by the product of two *power-conjugate* variables: effort, e, and flow, f, which are indicated above and below the power bond, respectively. Independent energy storage elements are identified by

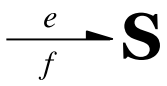

Figure 1: Element showing power bond and power conjugate variables

their relationships between their respective effort and flow variables. For an independent capacitive element, which represents potential energy storage, the effort, $e(t)$, is proportional to the integral of the flow, $f(t)$,

$$e(t) = \frac{1}{C}\,\mathbf{D}_t^{-1}[f(t)], \tag{1}$$

where C represents the capacitance of the element and $\mathbf{D}_t$ is a linear first-order differential operator with respect to time. Capacitive elements, designated by the symbol **C**, represent physical system components such as springs, electrical capacitors, and fluid columns in the presence of a gravitational field.

Taking the Laplace transform of both sides yields an expression for the effort, $E(s)$, in the frequency domain

$$\mathscr{L}(e(t)) = \mathscr{L}\left(\frac{1}{C}\,\mathbf{D}_t^{-1}[f(t)]\right) = E(s) = \frac{F(s)}{sC}. \tag{2}$$

Impedance is defined as the ratio of the effort to the flow, i.e.,

$$Z(s) = \frac{E(s)}{F(s)} \tag{3}$$

which leads to the expression for the impedance of a **C**-element,

$$Z_C(s) = (sC)^{-1}. \tag{4}$$

Similarly, for an independent inertive element, the flow is proportional to the integral of the effort,

$$f(t) = I\,\mathbf{D}_t^{-1}[e(t)] \tag{5}$$

where I represents the inertance of the element. Inertive elements, designated by the symbol **I**, represent physical system components such as masses, electrical inductors, and the mass of a fluid flowing through a pipe. The impedance of an inertive element is

$$Z_I(s) = sm. \tag{6}$$

A resistive element represents energy dissipation, where the effort and flow variables are directly proportional,

$$e(t) = R\, f(t). \tag{7}$$

The impedance of a resistive element is thus

$$Z_R(s) = R, \tag{8}$$

where R represents the resistance of the element. Resistive elements, designated by the symbol **R**, represent physical system components such as viscous dashpots and electrical resistors.

Parallel and series connections of elements in a mechanical system are represented in a bond graph using **1-** and **0-**junctions, respectively, as shown in Figure 2. Elements that experience the same force, or effort, and are connected via a **0-**junction, whereas all of elements that experience the same velocity, or flow, and are connected via a single **1-**junction. The relevant properties of junctions for impedance analyses presented here are: (a) the impedances of elements connected via a **1**-junction can be summed to form an equivalent impedance, Z_{eq}, and (b) the admittances, $Y = 1/Z$, of elements connected via a **0**-junction can be summed to form an equivalent admittance, Y_{eq}. Lastly, an externally applied forcing function to a system is represented in a bond graph by means of a *effort source* element, represented by the symbol **E**. Similarly, an externally imposed velocity is represented by a *flow source*, represented by the symbol **F**.

3. Fractional bond graph primitives in the frequency domain

Fractional Derivative Properties

Given that the Caputo definition (for its origins, see Caputo [5]), is recognized as being the more suitable choice for practical applications in the sciences and engineering, in comparison to others, such as the Riemann-Liouville and Grünwald-Letnikov definitions [11], it will be used exclusively in this application. Consider the frequency-domain behavior of the Caputo derivative, i.e., its Laplace transform on $[0, t]$,

$$\mathscr{L}\{\, {}_0^C\mathbf{D}_t^\alpha[f(t)]\,\} \;=\; s^\alpha F(s) \;-\; \sum_{k=0}^{n-1} s^{\alpha-k-1} f^{(k)}(0)\;,\quad (n-1 < \alpha \le n). \tag{9}$$

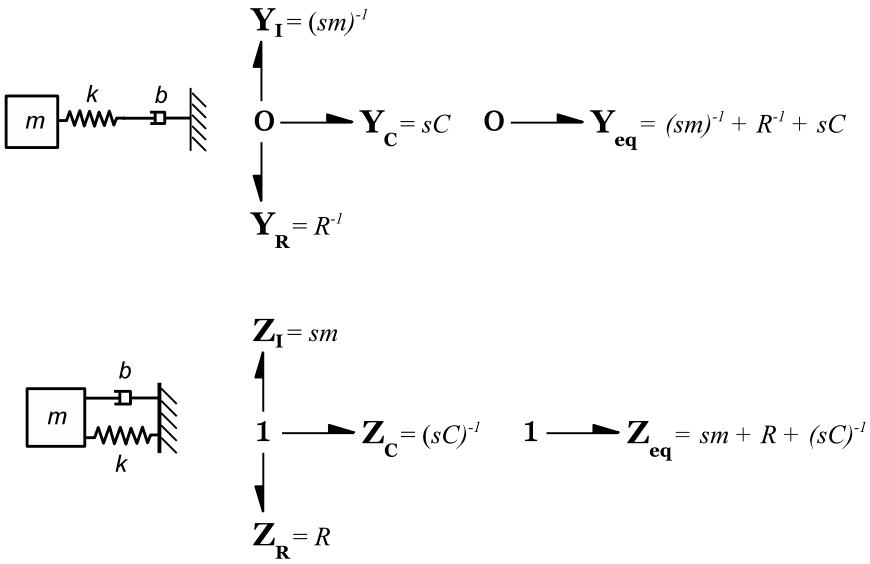

Figure 2: Equivalent impedance properties of junctions

The first term on the right-hand side of Equation (9) indicates a property of the fractional derivative that is significant to its application within the context of impedance-based bond graphs: α-order differentiation of a function, $f(t)$, corresponds to multiplication of its Laplace transform, $F(s)$, by s^α. In the interest of clarity and simplicity, only the superscript α and subscript t will be retained when denoting fractional differentiation with the operator $\mathbf{D}$.

Complex Plane Representation of Bond Graph Primitives

To aid in the visualization of impedance-based bond graph primitives, consider Figure 3, where the three integer-order primitive impedances are represented as phasors on the complex plane. Note that each differentiation with respect to time, i.e., multiplication by the complex frequency, s, represents an anti-clockwise rotation of the phasor by $\frac{\pi}{2}$.

Given that the fractional derivative operator, $\mathbf{D}^\alpha$, is a linear operator [11], one may be tempted to argue that an α^{th}-order differentiation, where $0 < \alpha < 1$, *could* be represented by an anti-clockwise rotation of the **C**-element phasor by $\frac{\alpha\pi}{2}$, yielding a new phasor $\mathbf{V_C}$ as shown in Figure 4. This would suggest that an impedance representation of a bond graph element

whose constitutive law contains a fractional derivative could be expressed as a combination of two primitive bond graph elements. We will show here that this is *not* the case, and that it indicates the need for primitive bond graph elements to represent physical phenomena that are accurately modeled using fractional derivatives [2], [11].

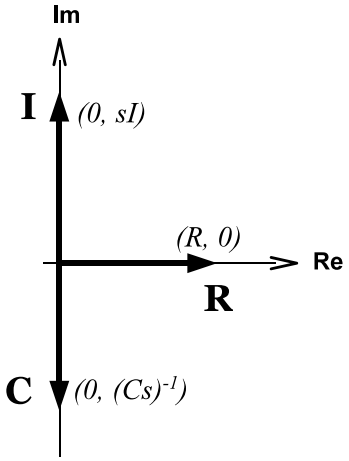

Figure 3: Primitive integer-order impedances on the complex plane

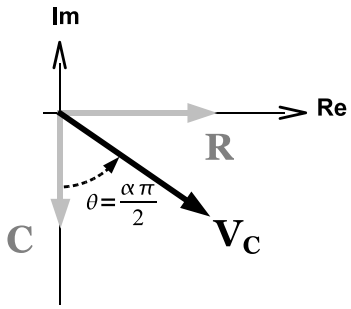

Figure 4: *Incorrect* conceptualization of a fractional-order viscoelastic primitive element, $\mathbf{V_C}$

It is clear that the phasor labeled $\mathbf{V_C}$ represents an impedance that exhibits both capacitive and resistive, i.e., viscoelastic, characteristics and that its equivalent impedance can be expressed as

$$Z_{VC} = R\,\cos\left(\frac{\alpha\pi}{2}\right) + \frac{\sin\left(\frac{\alpha\pi}{2}\right)}{(i\omega)C} = R\,\cos\left(\frac{\alpha\pi}{2}\right) + \frac{\sin\left(\frac{\alpha\pi}{2}\right)}{sC}. \qquad (10)$$

Note, however, that the impedance in Equation (10) is $\mathcal{O}(s^{-1})$, rather than $\mathcal{O}(s^{-\frac{1}{\alpha}})$ which would indicate the presence of a fractional derivative operator. Thus, the phasor $\mathbf{V_C}$ in Figure 4 represents an *integer-order* impedance and does not constitute a primitive impedance, since its impedance can be expressed in terms of a *finite* number of existing bond graph primitives.[1]

[1] *Ladder circuits*, which comprise a repetitive finite number of combinations of **R** and **C** elements, can be used to approximate viscoelastic behavior (and similarly, with **R** and **I** elements for viscoinertial behavior) will be shown later in this section to have significant shortcomings in certain practical applications.

Thus, we can conclude that fractional order impedances cannot be expressed in terms of existing bond graph primitive elements. Indeed, the complex-plane interpretation above suggests that an *infinite* number vector spaces would be necessary to represent all possible fractional-order impedances: one for each value of α where $\alpha \in \mathbb{R} : 0 < \alpha < 1$, i.e., for all possible orders of fractional differentiation.

To further support this argument, we present the equivalent impedances of well known constitutive models of linear viscoelasticity, i.e, Kelvin-Voigt, Maxwell, and Maxwell-Weichert models, of which the standard-linear model is a special case, where $n = 1$, as shown in Table 1. Inspection of these models reveals that their respective equivalent impedances are linear combinations of integer-order capacitive and resistive impedances, i.e., the complex frequency, s is raised to integer powers only; not to fractional powers, which would be indicative of an impedance that reflects fractional-order differentiation.

Kelvin-Voigt	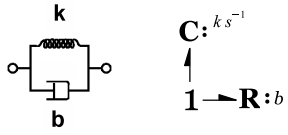	$Z_{eq} = \dfrac{sRC + 1}{sC}$
Maxwell	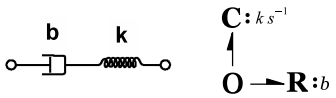	$Z_{eq} = \dfrac{R}{sRC + 1}$
Maxwell-Weichert	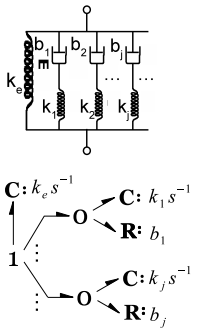	$Z_{eq} = \sum_{j=1}^{\infty} \dfrac{R_j}{R_j C_j s + 1}$

Table 1: Viscoelastic models

The above arguments support the assertion that a new primitive bond graph element which represents a fractional-order viscoelastic impedance is valid. Similar arguments can be made to support the notion of a primitive fractional-order viscoinertial impedance element, represented by the symbol $\mathbf{V_I}$.

Using Fractional Derivatives to Model Viscoelasticity

Having established the necessity for a primitive fractional-order viscoelastic impedance, we proceed with its application to a physical dynamical system. Bagley and Torvik, in their study of viscoelastic mountings for vibration damping in mechanical systems [1], as shown in Figure 5, determined that the relationship between the restoring force, f_p, of the material and its compression, x, is more accurately modeled with a constitutive law that features fractional differentiation rather than integer-order models based on those presented in Table 1, i.e.,

$$f_p(t) = \frac{2A}{\delta}\left(G_0 + G_1 \mathbf{D}_t^{\alpha}\right) x(t), \tag{11}$$

where $\mathbf{D}_t^{\alpha}$ is an α^{th}-order fractional differential operator, where $\alpha \in \mathbb{R} : 0 < \alpha < 1$. Taking the Laplace transform of both sides of Equation (11) and

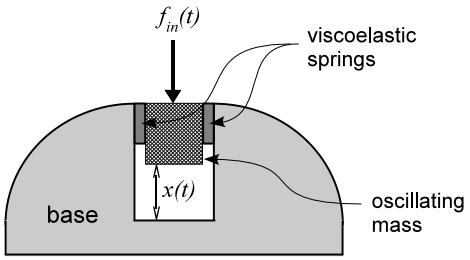

Figure 5: Viscoelastic mountings for a damped mechanical oscillator

assuming zero initial conditions yields

$$F_p(s) = \frac{2A}{\delta}\left(G_0 + G_1 s^{\alpha}\right) X(s). \tag{12}$$

Rearranging to form the ratio of the force to the velocity yields the equivalent impedance, Z_{eq} of the viscoelastic material

$$Z_{eq} = \frac{F_p(s)}{V(s)} = \frac{F_p(s)}{sX(s)} = \frac{2AG_0}{\delta} s^{-1} + \frac{2AG_1}{\delta} s^{\alpha-1}. \tag{13}$$

The impedance-based bond graph of the system of Figure 5 is shown in Figure 6, where the impedance of the first term of Equation 13 is modeled by a **C** element, i.e., an integer-order capacitive impedance, and is connected by a **1**-junction to the impedance of the second term, represented by the symbol, $\mathbf{V_C}$, whose impedance cannot be decomposed into terms with integer-order powers of s, i.e, a fractional-order viscoelastic impedance. The

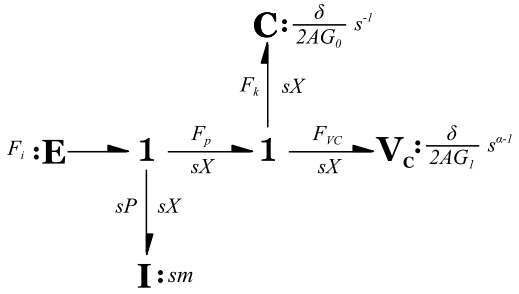

Figure 6: Bond graph model of vibration isolation system

dynamics of the system are described by the following system of differential equations in the *time domain*

$$\begin{aligned} \dot{p} &= F_i(t) - \frac{2AG_0}{\delta}x - \frac{2AG_1}{\delta}\mathbf{D}_t^{\alpha-1}[x] \\ \dot{x} &= \frac{p}{m}. \end{aligned} \tag{14}$$

The bond graph methodology provides a systematic procedure for extracting the state equations a dynamical system that would yield a system of coupled *first-order* ordinary differential equations, i.e., state equations,

$$\dot{\mathbf{x}} = \mathbf{A}\,\mathbf{x} + \mathbf{B}\,u(t). \tag{15}$$

However, the presence of the fractional-order primitive in the bond graph yields a coupled system that consists of a first-order ordinary differential equation and a fractional-order differential equation, which does not fit the generalized representation in Equation 15. A proposed solution method for this type of system of equations will be discussed in the next section. Before turning to this solution method, we present the application of the second proposed fractional-order bond graph primitive, which is used to model viscoinertial effects in a dynamical system.

Using Fractional Derivatives to Model Viscoinertial Effects

Consider the system where a spring, with stiffness k, is attached to a cylindrical mass, m, is immersed in a fluid with viscosity, μ, and density, ρ, as shown in Figure 7. The system is put into motion by an externally

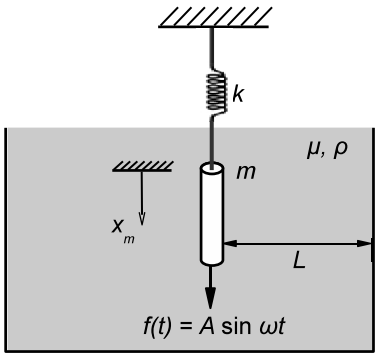

Figure 7: Immersed mass where the distance to the boundary, L, is large

applied forcing function, $f(t) = A \sin \omega t$. It is assumed that the distance between the mass and the boundary of the tank, L, is sufficiently large such that the assumption of a linear velocity profile of the fluid between the mass and the tank boundary becomes nonlinear. As the mass oscillates, the fluid near the boundary adheres to the mass, and stores kinetic energy. Thus, in addition to modeling the dissipative effects of the fluid, it is necessary to model the kinetic energy stored by the fluid that adheres to the mass.

One approach would be to model the fluid as a series of masses, M_j, where friction, approximated by a viscous constitutive law, is present between discrete fluid masses, as shown in Figure 8. This can be modeled using an explicit **I-R** *field* in the bond graph, using a series of primitive inertial and resistive elements, as shown in Figure 9. This approach is analogous to the use of *ladder circuits* in electrical system modeling, as alluded to earlier. This approach has a significant limitation: as the frequency of the excitation of the forcing function, ω, changes, the velocity profile of the fluid changes shape, which in turn affects the distribution of the discrete fluid masses, M_n and their corresponding velocities, v_i. Thus, the model is valid at a single frequency, or at best, a very narrow range of frequencies. Therefore, to accurately model this phenomenon for a wider range of frequencies would require a family of bond graph models, which would be unsuitable for practical applications. In a study of a vibration of a cylin-

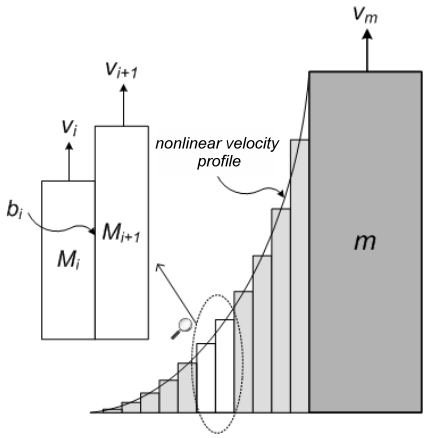

Figure 8: Schematic of fluid in motion using discrete masses

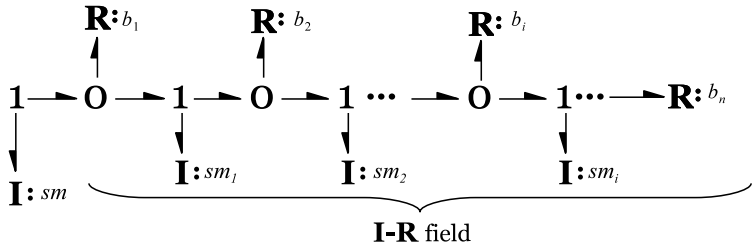

Figure 9: Discrete model of fluid motion and viscous effects

drical mass immersed in fluid, Bagley and Torvik [2] determined that the relationship between the drag force on the mass, f_d, and the velocity of mass, v_m, can be expressed using a fractional derivative

$$f_d = 2A\sqrt{\rho\mu}\ \ \mathbf{D}_t^{\frac{1}{2}}[v_m(t)], \tag{16}$$

where A is the surface area of the mass that is parallel to the direction of the velocity, and $\mathbf{D}^{\frac{1}{2}}$ is a half-order differential operator with respect to time. The presence of the fractional derivative operator captures the frequency-dependent effects of the viscoinertial phenomenon described previously, thus providing an alternative to the limitation of the **I-R** field modeling approach. Using a notation similar to that in the viscoelastic example in the previous section, the viscoinertial effects are represented by $\mathbf{V_I}$, in the bond graph of Figure 10. The causality of the bond leading into

$\mathbf{V_C}$ is fixed, since the constitutive law defined by Equation (16) is implicitly causal: the value of $v_m(t)$ is dependent on the velocity profile of the fluid, not the other way around. Thus, the effort is always defined by the flow. The state equations that model the behavior of this dynamical system are

$$\begin{aligned} \dot{x} &= \frac{p}{m}, \\ \dot{p} &= f(t) - kx - \frac{2A\sqrt{\rho\mu}}{m}\, \mathbf{D}_t^{\frac{1}{2}}\,[p]\,, \end{aligned} \tag{17}$$

where x is the displacement of the mass and p is the momentum of the mass. The presence of the fractional derivative term, due to the $\mathbf{V_I}$ element, in

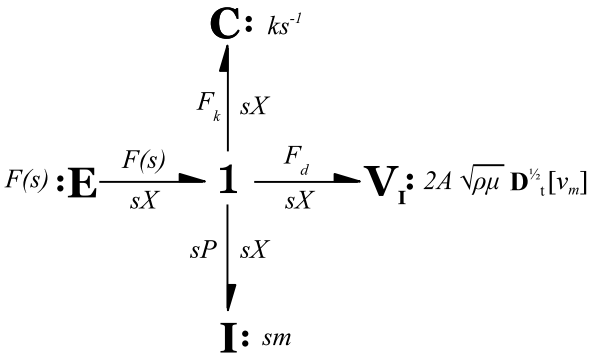

Figure 10: Bond graph with viscoinertial fractional-order element

the second equation yields a system of simultaneous *mixed* ordinary and fractional differential equations, as was seen with the viscoelastic example, i.e., Equation (14). Numerical solution methods for this type of equations will be examined in the next section.

4. Numerical solution of fractional-order differential equations

The analysis of the system in Section 2 performed by Bagley and Torvik [2] involves application of the non-homogeneous Bagley-Torvik equation, and a subsequent free-body diagram analysis, which yields a second-order differential equation that contains a fractional derivative,

$$\ddot{x} = f(t) - kx_m - 2A\sqrt{\rho\mu}\, \mathbf{D}_t^{\frac{1}{2}}\, v_m. \tag{18}$$

Their solution method for this equation introduced the notion of a *fractional* state space, in which a change of variables yields a state vector, $\mathbf{y}$, where *all*

of the state variables are expressed in terms of a half-order derivative. As an alternative solution, we propose to extend this representation to include systems of equations that contain fractional-order derivatives by introducing the notion of a partitioned vector of state variables,

$$\mathbf{x} = \left\{ \begin{array}{c} \mathbf{x_I} \\ \cdots \\ \mathbf{x_F} \end{array} \right\}, \tag{19}$$

where the partition x_I comprises the state variables that are subjected to integer-order differentiation only, and x_F comprises the state variables that are subjected to *both* fractional- and integer-order differentiation.

$$\dot{\mathbf{x}} = \mathbf{A} \left\{ \begin{array}{c} \mathbf{x_I} \\ \cdots \\ \mathbf{x_F} \end{array} \right\} + \mathbf{B}\, u(t) + \mathbf{\Phi}\, \mathbf{D}_t^{\alpha} \left[\left\{ \begin{array}{c} \mathbf{0} \\ \cdots \\ \mathbf{x_F} \end{array} \right\} \right]. \tag{20}$$

Equation (20) represents a *mixed state-space formulation* of the system of differential equations and thus suggests an approach where the fractional derivative of a state variable is explicitly computed, in comparison to the approach of Bagley et al [2], which involved implicit computation of fractional derivatives. Figure 11 illustrates this approach, where the differential equations are solved using an existing variable-step fourth-order Runge-Kutta algorithm which is linked to a subroutine that computes the fractional derivatives of the *necessary state variables only*, at each time step, t_i. This approach has several benefits: (1) it expands an existing paradigm, i.e.

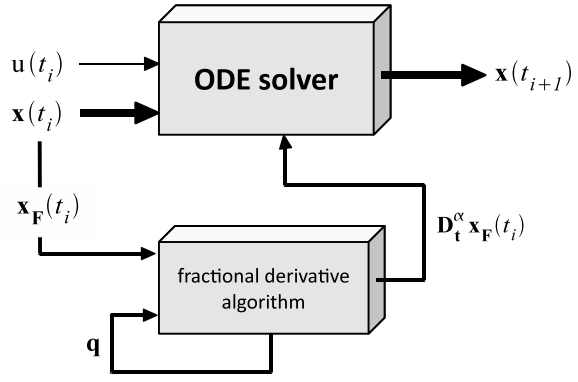

Figure 11: Numerical procedure

the state-space formulation, which is widely used in the modeling of state-determined systems, (2) it provides the dynamical system modeler with a

powerful tool to compute fractional derivatives without having to learn the complexities of fractional derivatives, i.e., it promotes more widespread use of fractional derivatives by making it accessible to those who would not otherwise attempt to use it, (3) it eliminates the need for a change of variables necessary for the implicit computation of fractional derivatives, which can become cumbersome as the number of state variables increases for more complex systems, and (4) it simplifies the computational process by explicitly computing fractional derivatives for system elements whose constitutive laws require it.

Numerical Simulation Results

In this section, we illustrate the validity and practical applicability of using fractional-order bond graph models and the accompanying numerical procedure borne from it. Of the various definitions of the fractional derivative presented in the literature [8], [11], the Caputo definition is cited as the most suitable for numerical computation [9] and is used for the simulations presented in this paper.

We return to the immersed cylindrical mass problem presented in Section 3. Examination of this problem will serve to validate that the mixed state-space approach yields valid results. It will also demonstrate its superiority to integer-order models in the analysis of complex physical phenomena, such as viscoinertial effects in physical dynamical systems.

We revisit the system of Figure 7, which is put into motion by an externally applied forcing function, $f(t) = A \sin \omega t$, and will compare the numerical results for both integer-order and fractional-order models of this system. The integer-order bond graph model for the system is shown in Figure 12. It features a primitive **R-**element, which implies that the drag force exerted by the mass on the fluid is purely resistive in nature and can be represented by viscous damping. The system of differential equations that describe the dynamics of this system are

$$\begin{aligned} \dot{x} &= \frac{p}{m}, \\ \dot{p} &= f(t) - kx - b\dot{x}. \end{aligned} \tag{21}$$

The fractional-order model is identical to that of Figure 10, where the drag force arises from both resistive and inertial effects, due to fluid adhering to the mass. The differential equations that describe the dynamics of the system are given in Equation (17). Given the frequency-dependent nature of the phenomenon that we wish to investigate, we seek to obtain plots of the frequency response of the system, where the input is the externally applied

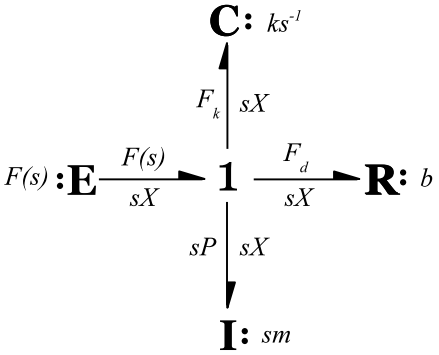

Figure 12: Integer-order model of immersed cylinder

forcing function, $f(t)$, and the output is the displacement of the mass, $x(t)$. The corresponding transfer function for the integer-order model is

$$T_i(s) = \frac{X(s)}{F(s)} = \frac{1}{s^2 m + bs + k}, \tag{22}$$

and the transfer function for the fractional-order model is

$$T_f(s) = \frac{X(s)}{F(s)} = \frac{1}{s^2 m + 2A\sqrt{\rho\mu}\, s^{\frac{3}{2}} + k}, \tag{23}$$

which are both obtained by taking the Laplace transform of Equations (21) and (17), respectively. The parameters of this system, shown in Figure 7, are: $m = 5$kg, $k = 1000$N/m, $\mu = 1.516$ N-s/m^2, $\rho = 898.4$kg/m^3, and $L = 2.15$m.

The equivalent viscous damping coefficient for the integer-order model, b, is calculated using the model parameters according to the following equation [3]

$$b = \frac{8\pi r^2 \ell^3 \mu}{L^4}, \tag{24}$$

where $r = 0.5$m and $\ell = 1.5$ m.

Simulations were run for both integer-order and fractional-order models where the frequency of the externally applied forcing function, $f(t)$, ranged from 1 - 100 rad/s. Figure 13 shows plots of the magnitude of the response, i.e., the displacement of the mass, vs. frequency, for both models. A plot of the relative error between these models, shown in Figure 14, reveals that the integer-order model does not sufficiently capture the viscoinertial effects in the 3–40 rad/s frequency range. The relative error varies with frequency:

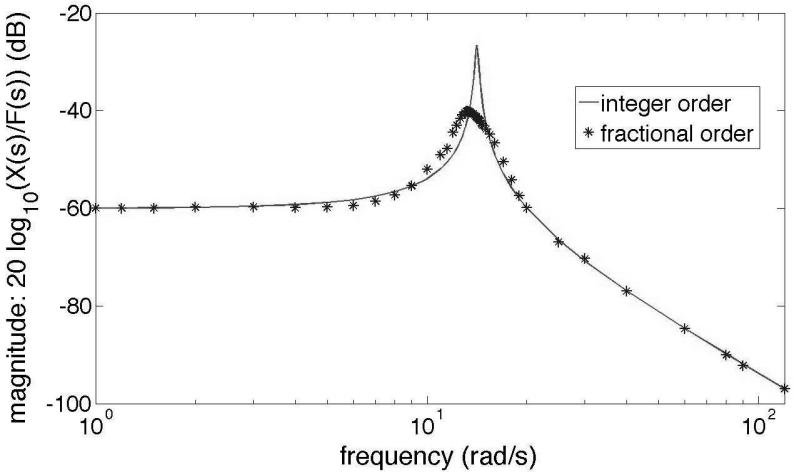

Figure 13: Comparison of frequency response for integer-order and fractional-order models

at frequencies up to 3 rad/s and above 40 rad/s, the error is approximately 0.5%. Within the 3–40 rad/s range, its average is approximately 20%, but reaches a maximum of over 420% in the vicinity of the resonant frequency at 13.2 rad/s. As indicated previously, the differences between simulated responses are attributable to fluid mass adhering to the cylindrical mass, resulting in kinetic energy storage, which is not provided for in the purely resistive **R** element in the integer-order model. Thus, we can conclude that the presence of the $\mathbf{V_I}$ element, with its fractional-order constitutive law, accounts for significant differences between the integer-order and fractional-order simulation results. Further, it is clear from Figure 13 that *both* the integer- and fractional-order models correctly predict the responses as $s \to 0$ and as $s \to \infty$, in accordance with Equations (22) and (23), i.e.,

$$\begin{aligned} \lim_{s\to 0} T_f(s) &= \frac{1}{k} = 0.001 = \text{-60 dB}, \\ \lim_{s\to \infty} T_f(s) &= 0. \end{aligned} \tag{25}$$

These results validate the mixed state-variable formulation and its accompanying numerical procedure put forth in this paper. These were a direct result of the formulation of new bond graph primitives that represent viscoinertial and viscoelastic phenomena observed in dynamical engineering systems.

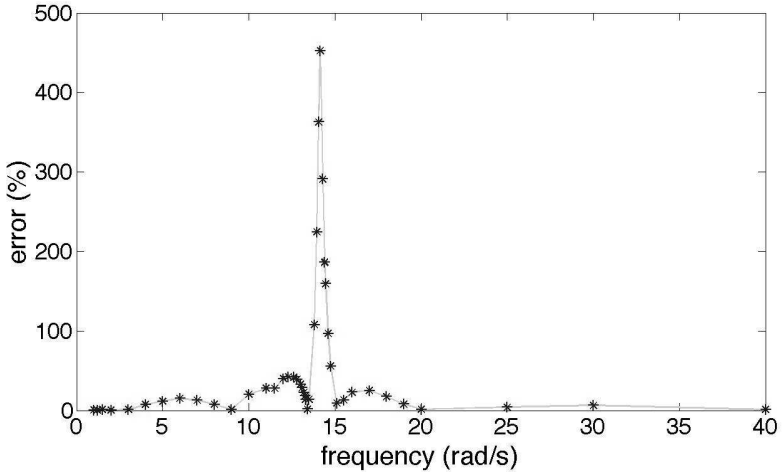

Figure 14: Percent error between integer-order and fractional-order models

5. Summary and conclusions

This paper introduced and proved the necessity of two new impedance-based bond graph primitives that represent physical phenomena whose constitutive laws are defined in terms of fractional derivatives. A new approach, borne out of notion of these primitive elements, that extended the state-space representation of dynamical systems to include simultaneous fractional and integer-order differential equations was presented. This approach was validated computationally by applying it to an engineering system that exhibits complex physical phenomena that are best represented mathematically using fractional differentiation.

References

[1] R.L. Bagley and P.J. Torvik, Fractional calculus - a different approach to the analysis of viscoelastically damped structures. *AIAA J. Applied Mechanics* **21** (1983), 741-748.

[2] R.L. Bagley and P.J. Torvik, On the appearance of the fractional derivative in the behavior of real materials. *J. Applied Mechanics* **51** (1984), 294-298.

[3] F.T. Brown, *Engineering System Dynamics: A Unified Graph-Centered Approach.* Marcel Dekker, Inc., New York, NY, 2001.

[4] I.J. Busch-Vishniac, *Electromechanical Sensors and Actuators*. Springer-Birkhäuser, Inc., New York, NY, 1999.

[5] M. Caputo, Linear models of dissipation whose Q is almost frequency independent. *Geophys. J. R. Astr. Soc.* **13** (1967), 529-539 (Reprinted recently in: *Fract. Calc. Appl. Anal.* **11**, No 1 (2008), 3-14).

[6] T.J. Connolly, J.A. Contreras, and R.L. Bagley, New bond graph primitive elements for systems modeled by fractional derivatives. *Proc. of IMECE 2006: Intern. Mechanical Engineering Congress and Exposition*, American Soc. of Mechanical Engineers, Chicago, IL, Nov. 2006.

[7] J. Contréras, *New Bond Graph Elements for Systems Modeled by Fractional Derivatives*. Master Thesis, Univ. of Texas at San Antonio, 2006.

[8] K. Diethelm, N.J. Ford, A.D. Freed, and Y. Luchko, Algorithms for the fractional calculus: a selection of numerical methods. *Computer Methods in Appl. Mechanics and Engineering* **94** (2005), 743-777.

[9] D. Elliott, An asymptotic analysis of two algorithms for certain Hadamard finite-part integrals. *IMA J. Numer. Anal.* **13** (1993), 445-467.

[10] D. Karnopp, D. Margolis, and R. Rosenberg, *System Dynamics: Modeling and Control of Mechatronic Systems*. J. Wiley and Sons, Hoboken, NJ, 3d Ed., 2006.

[11] I. Podlubny, *Fractional Differential Equations*. Academic Press, San Diego, CA, 1999.

[1] *Dept. of Mechanical Engineering*
The University of Texas at San Antonio
1 UTSA Circle, EB 3.04.24, San Antonio, TX 78249 – U.S.A.
e-mail: thomas.connolly@utsa.edu

Received: May 26, 2009

[2] *Dept. of Aerospace Engineering*
Universidád Autónoma de Chihuahua
Av. Escorza No. 900, Zona Centro, CP. 31000, Chihuahua – MÉXICO
e-mail: jaimeac22@gmail.com